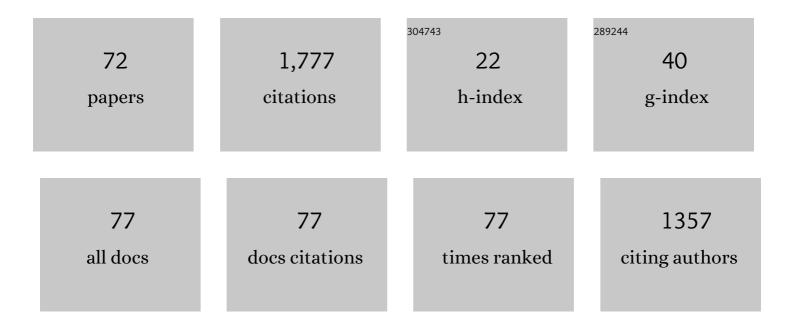


List of Publications by Year in descending order

Source: https://exaly.com/author-pdf/914300/publications.pdf Version: 2024-02-01



CADV RUST

#	Article	IF	CITATIONS
1	History, current state, and future directions of ionospheric imaging. Reviews of Geophysics, 2008, 46, .	23.0	210
2	lonospheric Data Assimilation Three-Dimensional (IDA3D): A global, multisensor, electron density specification algorithm. Journal of Geophysical Research, 2004, 109, .	3.3	180
3	The Ionospheric Connection Explorer Mission: Mission Goals and Design. Space Science Reviews, 2018, 214, 1.	8.1	152
4	Global thermosphere-ionosphere response to onset of 20 November 2003 magnetic storm. Journal of Geophysical Research, 2006, 111, .	3.3	105
5	Intelligent systems for geosciences. Communications of the ACM, 2018, 62, 76-84.	4.5	71
6	Two-dimensional mapping of the plasma density in the upper atmosphere with computerized ionospheric tomography (CIT). Physics of Plasmas, 1998, 5, 2010-2021.	1.9	54
7	Four-dimensional GPS imaging of space weather storms. Space Weather, 2007, 5, n/a-n/a.	3.7	53
8	Ionospheric data assimilation and forecasting during storms. Journal of Geophysical Research: Space Physics, 2016, 121, 764-778.	2.4	51
9	Tracking of polar cap ionospheric patches using data assimilation. Journal of Geophysical Research, 2007, 112, n/a-n/a.	3.3	49
10	lonospheric scintillation over Antarctica during the storm of 5–6 April 2010. Journal of Geophysical Research, 2012, 117, .	3.3	45
11	GPS phase scintillation associated with optical auroral emissions: First statistical results from the geographic South Pole. Journal of Geophysical Research: Space Physics, 2013, 118, 2490-2502.	2.4	45
12	Combined Ionospheric Campaign 1: Ionospheric tomography and GPS total electron count (TEC) depletions. Geophysical Research Letters, 2000, 27, 2849-2852.	4.0	43
13	Satelliteâ€beacon Ionosphericâ€scintillation Global Model of the upper Atmosphere (SIGMA) I: Highâ€latitude sensitivity study of the model parameters. Journal of Geophysical Research: Space Physics, 2014, 119, 4026-4043.	2.4	40
14	C/NOFS observations of intermediate and transitional scale-size equatorial spreadFirregularities. Geophysical Research Letters, 2009, 36, .	4.0	31
15	Observed and modeled thermosphere and ionosphere response to superstorms. Radio Science, 2007, 42, .	1.6	30
16	Identification of scintillation signatures on GPS signals originating from plasma structures detected with EISCAT incoherent scatter radar along the same line of sight. Journal of Geophysical Research: Space Physics, 2017, 122, 916-931.	2.4	28
17	Satelliteâ€beacon Ionosphericâ€scintillation Global Model of the upper Atmosphere (SIGMA) II: Inverse modeling with highâ€latitude observations to deduce irregularity physics. Journal of Geophysical Research: Space Physics, 2016, 121, 9188-9203.	2.4	26
18	Tomographic studies of aeronomic phenomena using radio and UV techniques. Journal of Atmospheric and Solar-Terrestrial Physics, 2002, 64, 1573-1580.	1.6	25

GARY BUST

#	Article	IF	CITATIONS
19	High-latitude plasma structure and scintillation. Radio Science, 2004, 39, n/a-n/a.	1.6	25
20	Estimating <i>E</i> region density profiles from radio occultation measurements assisted by IDA4D. Journal of Geophysical Research, 2009, 114, .	3.3	25
21	IRI data ingestion and ionospheric tomography. Advances in Space Research, 2001, 27, 157-165.	2.6	22
22	Radio tomographic imaging of sporadic- <i>E</i> layers during SEEK-2. Annales Geophysicae, 2005, 23, 2357-2368.	1.6	22
23	Ionospheric observations of the November 1993 storm. Journal of Geophysical Research, 1997, 102, 14293-14304.	3.3	21
24	Initial GPS scintillation results from CASES receiver at South Pole, Antarctica. Radio Science, 2012, 47,	1.6	21
25	First light from a kilometerâ€baseline Scintillation Auroral GPS Array. Geophysical Research Letters, 2015, 42, 3639-3646.	4.0	21
26	Application of ionospheric tomography to single-site location range estimation. International Journal of Imaging Systems and Technology, 1994, 5, 160-168.	4.1	19
27	Observations of the F region height redistribution in the storm-time ionosphere over Europe and the USA using GPS imaging. Geophysical Research Letters, 2006, 33, n/a-n/a.	4.0	19
28	Neutral wind estimation from 4â $\!\!\in\!\!$ D ionospheric electron density images. Journal of Geophysical Research, 2009, 114, .	3.3	18
29	Effects of solar cycle 24 activity on WAAS navigation. Space Weather, 2014, 12, 46-63.	3.7	18
30	Mid-America Computerized Ionospheric Tomography Experiment (MACE '93). Radio Science, 1995, 30, 105-108.	1.6	17
31	Computerized ionospheric tomography analysis of the Combined Ionospheric Campaign. Radio Science, 2001, 36, 1599-1605.	1.6	16
32	Verification of ionospheric sensors. Radio Science, 2001, 36, 1523-1529.	1.6	15
33	lonospheric data assimilation applied to HF geolocation in the presence of traveling ionospheric disturbances. Radio Science, 2017, 52, 829-840.	1.6	15
34	Evidence for the tongue of ionization under northward interplanetary magnetic field conditions. Journal of Geophysical Research, 2005, 110, .	3.3	14
35	Recent results of the CEDAR storm study. Advances in Space Research, 1997, 20, 1655-1664.	2.6	13
36	Deducing storm time <i>F</i> region ionospheric dynamics from 3-D time-varying imaging. Journal of Geophysical Research, 2011, 116, .	3.3	13

GARY BUST

#	Article	IF	CITATIONS
37	Distributed sensing of ionospheric irregularities with a GNSS receiver array. Radio Science, 2017, 52, 988-1003.	1.6	13
38	Amplitudes and wavelengths of wavy Taylor vortices. Physics of Fluids, 1985, 28, 1243.	1.4	12
39	Modeled and observed equatorial thermospheric winds and temperatures. Journal of Geophysical Research: Space Physics, 2015, 120, 5832-5844.	2.4	11
40	Threeâ€dimensional modeling of highâ€latitude scintillation observations. Radio Science, 2016, 51, 1022-1029.	1.6	11
41	First stormâ€time plasma velocity estimates from highâ€resolution ionospheric data assimilation. Journal of Geophysical Research: Space Physics, 2013, 118, 7458-7471.	2.4	10
42	lonospheric irregularities during a substorm event: Observations of ULF pulsations and GPS scintillations. Journal of Atmospheric and Solar-Terrestrial Physics, 2014, 114, 1-8.	1.6	10
43	IDA4D: Ionospheric Data Assimilation for the ICON Mission. Space Science Reviews, 2020, 216, 1.	8.1	10
44	An interhemispheric comparison of GPS phase scintillation with auroral emission observed at the South Pole and from the DMSP satellite. Annals of Geophysics, 2013, 56, .	1.0	10
45	Variations in the midlatitude and equatorial ionosphere during the October 2003 magnetic storm. Radio Science, 2006, 41, n/a-n/a.	1.6	9
46	Radio tomographic imaging of the northern high-latitude ionosphere on a wide geographic scale. Radio Science, 2005, 40, n/a-n/a.	1.6	8
47	Global observations of <i>E</i> region plasma density morphology and variability. Journal of Geophysical Research, 2012, 117, .	3.3	8
48	GEOScan: A global, real-time geoscience facility. , 2013, , .		8
49	Tomographic Imaging of Traveling Ionospheric Disturbances Using GNSS and Geostationary Satellite Observations. Journal of Geophysical Research: Space Physics, 2020, 125, e2019JA027551.	2.4	7
50	Were the Lyman-alpha clouds formed from shocks?. Astrophysical Journal, 1987, 319, 14.	4.5	7
51	Assimilation of thermospheric measurements for ionosphereâ€ŧhermosphere state estimation. Radio Science, 2016, 51, 1818-1837.	1.6	6
52	Nightâ€īime Ionospheric Localized Enhancements (NILE) Observed in North America Following Geomagnetic Disturbances. Journal of Geophysical Research: Space Physics, 2021, 126, e2021JA029324.	2.4	6
53	LOFAR as an ionospheric probe. Planetary and Space Science, 2004, 52, 1375-1380.	1.7	5
54	Mapping the Time-Varying Distribution of High-Altitude Plasma During Storms. Geophysical Monograph Series, 0, , 91-98.	0.1	5

GARY BUST

#	Article	IF	CITATIONS
55	Development and error analysis of nonlinear ionospheric removal algorithm for ionospheric electron density determination using broadband RF data. Journal of Geophysical Research, 2011, 116, n/a-n/a.	3.3	5
56	Mapping plasma structures in the high-latitude ionosphere using beacon satellite, incoherent scatter radar and ground-based magnetometer observations. Annals of Geophysics, 2009, 45, .	1.0	5
57	A novel data assimilation technique for the plasmasphere. Journal of Geophysical Research: Space Physics, 2015, 120, 8470-8485.	2.4	4
58	Estimating Height and Thickness of an Ionospheric Irregularity Layer with a Closely-Spaced GNSS Receiver Array. , 0, , .		4
59	GEOScan: a geoscience facility from space. Proceedings of SPIE, 2012, , .	0.8	2
60	lonospheric Irregularity Layer Height and Thickness Estimation With a GNSS Receiver Array. IEEE Transactions on Geoscience and Remote Sensing, 2021, 59, 6198-6207.	6.3	2
61	The Coherent Electromagnetic Radio Tomography (CERTO) experiment on ARGOS. , 2001, , .		1
62	Assimilation of GNSS Measurements for Estimation of High‣atitude Convection Processes. Space Weather, 2020, 18, e2019SW002409.	3.7	1
63	Auroral E and F Layer Ionospheric Irregularities Sensed by a Kilometer-Spaced GNSS Receiver Array. , 0, ,		1
64	Properties of high latitude irregularities with a short-baseline 2D GPS scintillation array. , 2014, , .		0
65	Inferring 2D spatio-temporal properties of irregularities from a closely-spaced sub-auroral scintillation array. , 2014, , .		0
66	Community-wide model validation study for systematic assessment of ionosphere models. , 2015, , .		0
67	lonospheric-thermospheric state estimation with neutral wind data assimilation. , 2015, , .		0
68	Inverse modeling of ionospheric irregularities observed using GPS scintillations at Poker Flat, AK. , 2017, , .		0
69	Identifying E and F Region Irregularities with a Scintillation Auroral GPS Array. , 2018, , .		0
70	Auroral Ionospheric Irregularity Properties via Estimation and Inverse Modeling of GNSS Scintillations. , 2019, , .		0
71	A Night-time lonospheric Localized Enhancement (NILE) During Extreme Storms. , 0, , .		0
72	Tomographic imaging of a large-scale travelling ionospheric disturbance during the Halloween storm of 2003. Annales Geophysicae, 2020, 38, 1149-1157.	1.6	0